

# Polo-like kinase 4 kinase activity limits centrosome overduplication by autoregulating its own stability

Andrew J. Holland,<sup>1,2</sup> Weijie Lan,<sup>1,2</sup> Sherry Niessen,<sup>3,4</sup> Heather Hoover,<sup>3,4</sup> and Don W. Cleveland<sup>1,2</sup>

<sup>1</sup>Ludwig Institute for Cancer Research and <sup>2</sup>Department of Cellular and Molecular Medicine, University of California, San Diego, La Jolla, CA 92093

<sup>3</sup>The Skaggs Institute for Chemical Biology and <sup>4</sup>Department of Chemical Physiology, The Center for Physiological Proteomics, The Scripps Research Institute, La Jolla, CA 92037

**A**ccurate control of the number of centrosomes, the major microtubule-organizing centers of animal cells, is critical for the maintenance of genome integrity. Abnormalities in centrosome number can promote errors in spindle formation that lead to subsequent chromosome missegregation, and extra centrosomes are found in many cancers. Centrosomes are comprised of a pair of centrioles surrounded by amorphous pericentriolar material, and centrosome duplication is controlled by centriole replication. Polo-like kinase 4 (Plk4) plays a key role in initiating centriole duplication, and over-

expression of Plk4 promotes centriole overduplication and the formation of extra centrosomes. Using chemical genetics, we show that kinase-active Plk4 is inherently unstable and targeted for degradation. Plk4 is shown to multiply self-phosphorylate within a 24-amino acid phosphodegron. Phosphorylation of multiple sites is required for Plk4 instability, indicating a requirement for a threshold level of Plk4 kinase activity to promote its own destruction. We propose that kinase-mediated, autoregulated instability of Plk4 self-limits Plk4 activity so as to prevent centrosome amplification.

## Introduction

Centrosomes are the major microtubule-organizing centers of animal cells and play an important role in organizing the interphase cytoskeleton and poles of the mitotic spindle (Nigg, 2002). A single centrosome is comprised of a pair of centrioles surrounded by an amorphous pericentriolar material, and centrosome duplication is controlled by centriole replication (Loncarek and Khodjakov, 2009). In dividing cells, centrioles duplicate once per cell cycle adjacent to preexisting centrioles. Errors in this process lead to the production of an abnormal centrosome number that can promote errors in spindle formation and subsequent chromosome missegregation (Ganem et al., 2009; Silkworth et al., 2009). Moreover, abnormalities in centrosome number are often observed in cancer cells; and thus, accurate control of centrosome number is critical for the maintenance of genome integrity (Nigg, 2006; Holland and Cleveland, 2009).

Centriole duplication is regulated by the conserved protein kinase Polo-like kinase 4 (Plk4; also known as SAK). Overexpression of Plk4 overrides the mechanism that limits

centriole duplication, leading to multiple rounds of centriole duplication within a single cell cycle (Bettencourt-Dias et al., 2005; Habadanck et al., 2005; Peel et al., 2007; Basto et al., 2008). Plk4 is aberrantly expressed in human colorectal and liver cancer (Macmillan et al., 2001; Ko et al., 2005). Furthermore, Plk4<sup>+/-</sup> mice develop spontaneous liver and lung tumors (Ko et al., 2005), whereas overexpression of Plk4 promotes centrosome amplification and tumorigenesis in flies (Basto et al., 2008; Castellanos et al., 2008). Therefore, Plk4 activity must be precisely regulated to accurately control centriole duplication and prevent transformation.

Plk4 is a low abundance protein with a short cellular half-life (Fode et al., 1996). Plk4 is ubiquitinated and degraded by the 26S proteasome (Fode et al., 1996; Cunha-Ferreira et al., 2009; Korzeniewski et al., 2009; Rogers et al., 2009), and inhibiting proteasome function promotes centriole overduplication in a Plk4-dependent manner (Duensing et al., 2007). The SKP1-CUL1-F Box (SCF) complex is an E3 ubiquitin ligase comprised of three core subunits (Skp1, Cullin 1, and Rbx1) and

Correspondence to Don W. Cleveland: [dcleveland@ucsd.edu](mailto:dcleveland@ucsd.edu)

Abbreviations used in this paper: AS, analogue sensitive; Flp, flippase; FRT, Flp recombination target; GBP, GFP-binding protein; KD, kinase dead; LPC, leupeptin, pepstatin, and chymostatin; MS, mass spectrometry; Plk4, Polo-like kinase 4; SCF, SKP1-CUL1-F Box; WT, wild type.

© 2010 Holland et al. This article is distributed under the terms of an Attribution-Noncommercial-Share Alike-No Mirror Sites license for the first six months after the publication date (see <http://www.jcb.org/misc/terms.shtml>). After six months it is available under a Creative Commons License (Attribution-Noncommercial-Share Alike 3.0 Unported license, as described at <http://creativecommons.org/licenses/by-nc-sa/3.0/>).

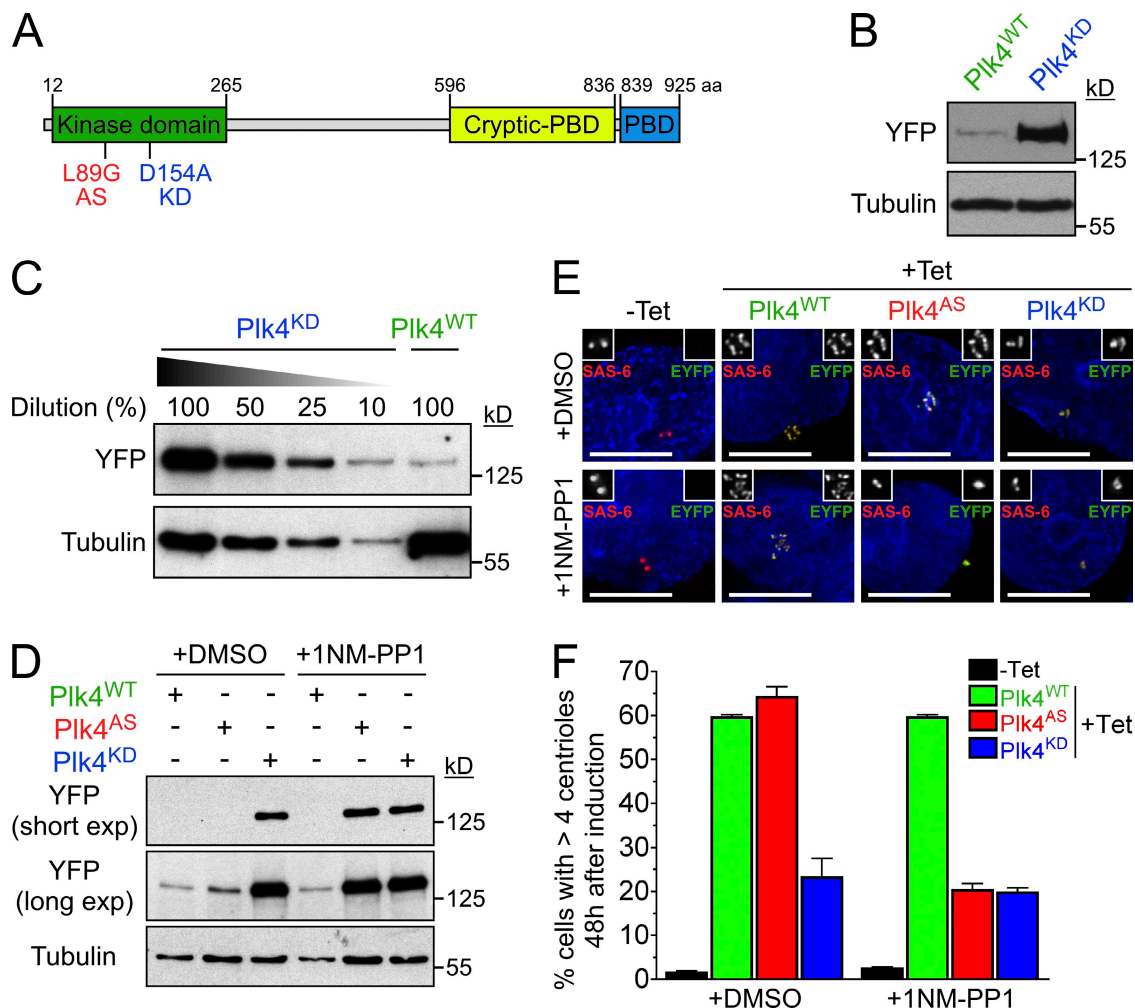


**Figure 1. Plk4 kinase activity destabilizes the protein.** (A) Schematic of mouse Plk4, showing the location of the kinase domain, the Polo-box domain (PBD), and the cryptic Polo-box domain (Swallow et al., 2005). The locations of the AS and KD mutations are also shown. (B) Immunoblot showing the expression level of WT and KD Plk4-EYFP transgenes. (C) Titration showing the relative expression level of Plk4<sup>WT</sup> and Plk4<sup>KD</sup>. (D) Immunoblot showing the expression levels of Plk4<sup>WT</sup>, Plk4<sup>AS</sup>, and Plk4<sup>KD</sup> in the presence of DMSO or 1NM-PP1. (E) Immunofluorescence images acquired 48 h after Plk4-EYFP was induced with tetracycline. Cells were grown in DMSO or 1NM-PP1. Insets depict an enlargement of centrioles. Red, SAS-6; green, Plk4-EYFP; blue, DNA. Bars, 10  $\mu$ m. (F) Graph quantifying the proportion of cells with more than four centrioles 48 h after expression of Plk4-EYFP was induced. Cells were grown in the presence of either DMSO or 1NM-PP1. Bars represent the mean of at least three independent experiments with >300 cells per condition. Error bars represent the SEM.

a variable F box protein that recognizes substrates only when they are phosphorylated at specific sites (Frescas and Pagano, 2008). In *Drosophila melanogaster* cells, the SCF F box protein Slimb prevents centrosome amplification by ubiquitinating and promoting the degradation of SAK/Plk4 (Cunha-Ferreira et al., 2009; Rogers et al., 2009). A direct role of  $\beta$ -TrCP (the vertebrate homologue of *Drosophila* Slimb) in promoting the destruction of Plk4 has not been demonstrated in vertebrates, although mouse cells lacking  $\beta$ -TrCP have excess centrosomes (Guardavaccaro et al., 2003). In this study, we investigate the mechanism that limits Plk4 levels in vertebrates and show that Plk4 stability is regulated by its own kinase activity.

## Results and discussion

To determine how mammalian Plk4 levels are established, EYFP-tagged wild-type (WT) and kinase-inactive (D154A) mouse

Plk4 (Fig. 1 A) were stably expressed in a human cell line (DLD-1) in which accurate chromosome segregation maintains a pseudodiploid karyotype (Lengauer et al., 1997). To facilitate direct comparison, WT and kinase-dead (KD) Plk4-EYFP transgenes were integrated at a predefined genomic locus in the host cell line using flippase (Flp) recombination target (FRT)/Flp-mediated recombination. Plk4-EYFP expression was under tight tetracycline regulation, allowing temporal control of Plk4 kinase-induced centriole biogenesis (Fig. S1, A and C). Previous work has shown that overexpressed Plk4<sup>KD</sup> can increase centrosome numbers in cycling populations of cells, whereas Plk4<sup>WT</sup> promotes centrosome amplification in S phase-arrested cells (Habadanck et al., 2005), suggesting dual pathways (one kinase dependent and another that is kinase independent) for Plk4 stimulation of centrosome duplication. Indeed, 48 h after induction of Plk4<sup>WT</sup>, 60% of asynchronously growing cells showed evidence of centriole amplification, whereas induction

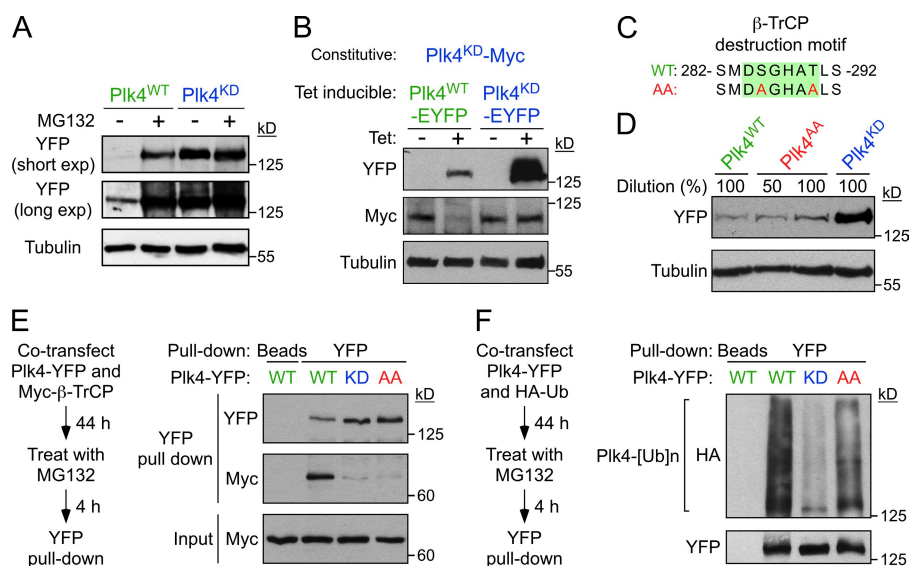


**Figure 2. Phosphorylation of the  $\beta$ -TrCP-binding motif has a minor effect on the stability of mouse Plk4.** (A) Cells were treated with or without the proteasome inhibitor MG132 for 8 h and immunoblotted to determine the expression level of Plk4<sup>WT</sup> and Plk4<sup>KD</sup>. (B) Expression of Plk4<sup>WT</sup>-EYFP or Plk4<sup>KD</sup>-EYFP was induced for 24 h in cells constitutively expressing Plk4<sup>KD</sup>-Myc. The expression level of the Myc and EYFP-tagged Plk4 transgenes was subsequently determined by immunoblotting. (C) The Plk4<sup>AA</sup> mutant possesses two mutations that prevent phosphorylation of the  $\beta$ -TrCP-binding motif (highlighted in green). (D) Immunoblot shows a modest increase in the stability of Plk4<sup>AA</sup>. (E) HEK 293 cells were cotransfected with Plk4-EYFP and Myc- $\beta$ -TrCP and treated with MG132 for 4 h. Plk4-EYFP was purified using GBP-coupled beads or beads alone, and protein complexes were analyzed by immunoblotting. (F) HEK 293 cells were cotransfected with Plk4-EYFP and HA-ubiquitin and treated with MG132 for 4 h. Plk4-EYFP was purified using GBP-coupled beads or beads alone, and protein complexes were analyzed by immunoblotting.

of Plk4<sup>KD</sup> caused centriole amplification in a 2.5-fold smaller proportion (23%) of cells (Fig. 1, E and F; and Fig. S1 B).

Surprisingly, the total level of Plk4<sup>KD</sup> protein was >10-fold higher than that of Plk4<sup>WT</sup> (Fig. 1, B and C), and the level of Plk4<sup>KD</sup> at the centriole was >45-fold higher than that of Plk4<sup>WT</sup> (Fig. S1, D and E), implicating kinase activity of Plk4 as a determinant of its stability. To test this hypothesis, we created an ATP analogue-sensitive (AS) mutant of Plk4 (Bishop et al., 2000). Plk4<sup>AS</sup> possesses a point mutation at a conserved gatekeeper residue (L89G) that enlarges the ATP-binding pocket and allows the kinase to be selectively inhibited by the bulky ATP analogue 1NM-PP1 (Fig. 1 A). To characterize the Plk4<sup>AS</sup> allele, we expressed and purified recombinant WT, AS, and KD GST-Plk4 and tested the ability of the kinase to phosphorylate histone H1 in vitro. GST-Plk4<sup>WT</sup> phosphorylated itself (in cis or trans) and the substrate histone H1, whereas GST-Plk4<sup>KD</sup> lacked detectable activity (Fig. S2, A and B). In comparison with GST-Plk4<sup>WT</sup>, GST-Plk4<sup>AS</sup> exhibited an  $\sim$ 2.5 reduction in phosphorylation of itself and an  $\sim$ 10-fold reduction in phosphorylation of the histone H1 (Fig. S2, A and C), which are reductions comparable with that observed with a similar Plk1<sup>AS</sup> allele that was shown to compensate for the loss of endogenous Plk1 in cells (Burkard et al., 2007).

As expected, in vitro 1NM-PP1 inhibited the activity of GST-Plk4<sup>AS</sup> but not GST-Plk4<sup>WT</sup> (Fig. S2 C). Therefore, we created stable cell lines expressing Plk4<sup>AS</sup>-EYFP and examined Plk4's stability and ability to promote centriole amplification in the presence or absence of the 1NM-PP1. In the absence of drugs Plk4<sup>AS</sup> was expressed at a low level that promoted centriole overduplication in 64% of cells, which is similar to that observed with Plk4<sup>WT</sup> (Fig. 1, D–F). In contrast, addition of 1NM-PP1 caused a dramatic increase in the abundance of Plk4<sup>AS</sup> and reduced centriole overduplication to the level observed with Plk4<sup>KD</sup> (Fig. 1, D–F). This suggests that the activity of Plk4<sup>AS</sup> can be inhibited by 1NM-PP1 in vivo and confirms that Plk4 kinase activity regulates its own stability.

The 26 S proteasome inhibitor MG132 was added to Plk4<sup>WT</sup>- and Plk4<sup>KD</sup>-expressing cells to determine whether Plk4 kinase activity promotes proteasome-mediated Plk4 destruction. Plk4<sup>WT</sup> but not Plk4<sup>KD</sup> was substantially stabilized by MG132 treatment (Fig. 2 A). To determine whether kinase-active Plk4 is capable of destabilizing Plk4<sup>KD</sup> in trans, we induced expression of Plk4<sup>WT</sup>-EYFP or Plk4<sup>KD</sup>-EYFP in cells constitutively expressing Plk4<sup>KD</sup>-Myc. Expression of Plk4<sup>WT</sup>-EYFP, but not Plk4<sup>KD</sup>-EYFP, reduced the stability of Plk4<sup>KD</sup>-Myc, demonstrating that Plk4 can promote self-destruction through intermolecular phosphorylation (Fig. 2 B).

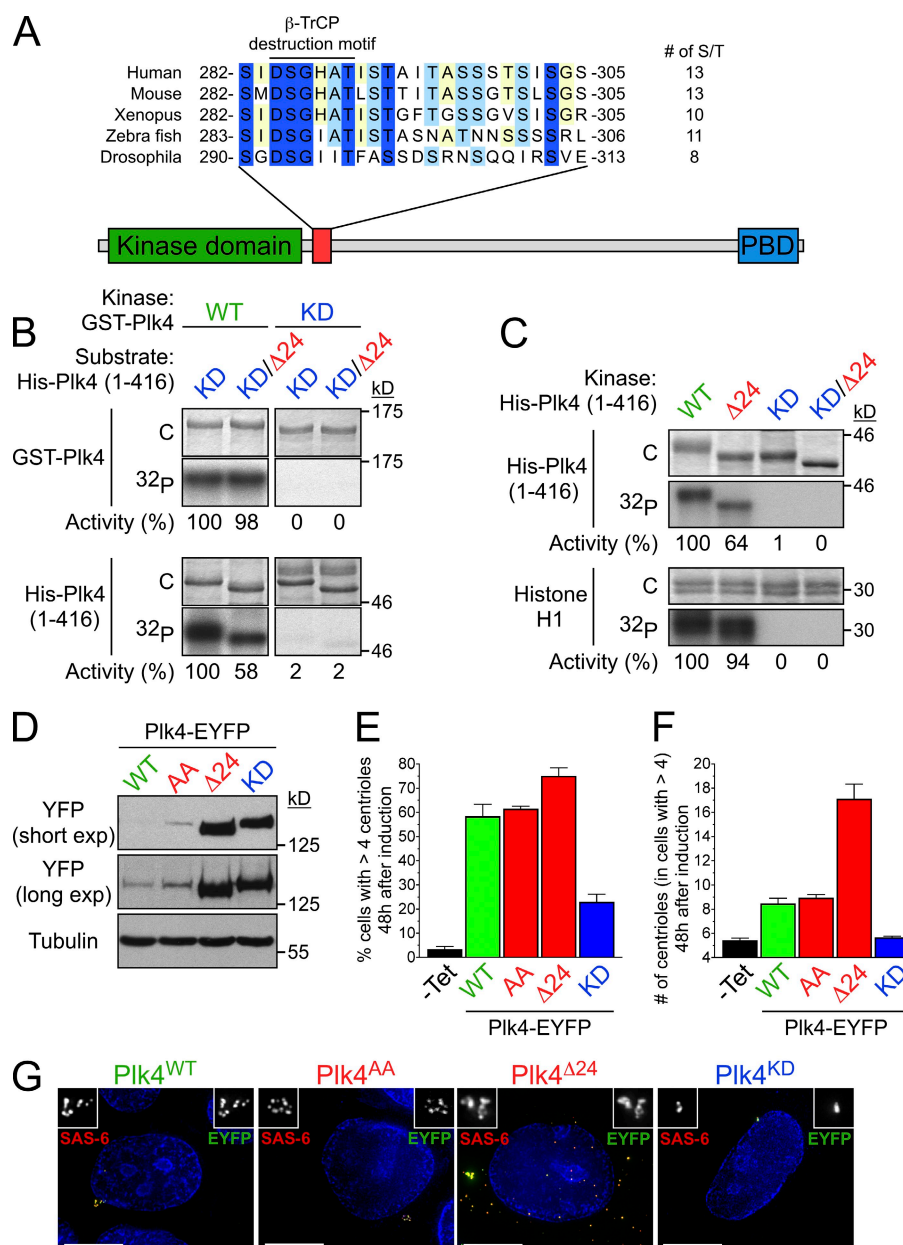
Our data support a model in which autophosphorylation triggers Plk4's destruction to self-limit kinase activity. Plk4 possesses a conserved SCF <sup>$\beta$ -TrCP</sup> phosphodegron, and previous studies in *Drosophila* cells have implicated a role of this two-phosphosite phosphodegron in regulating Plk4's stability (Cunha-Ferreira et al., 2009; Rogers et al., 2009). Therefore, we considered the possibility that autophosphorylation (in cis or trans) of the  $\beta$ -TrCP phosphodegron was required for Plk4 to promote its own destruction. To test this hypothesis, we created a mutant Plk4 in which both phosphorylation sites in the  $\beta$ -TrCP destruction motif were mutated to alanine (Plk4<sup>AA</sup>; Fig. 2 C). Plk4<sup>AA</sup> and Plk4<sup>KD</sup> both showed a dramatic reduction in  $\beta$ -TrCP binding, which is consistent with Plk4 autophosphorylation of the  $\beta$ -TrCP destruction motif in promoting  $\beta$ -TrCP binding (Fig. 2 E). However, in contrast to Plk4<sup>KD</sup>, Plk4<sup>AA</sup> was ubiquitinated (albeit at a reduced level compared with Plk4<sup>WT</sup>) in cells (Fig. 2 F) and was only about twofold more stable than Plk4<sup>WT</sup> (Fig. 2 D). This demonstrates that phosphorylation of the  $\beta$ -TrCP destruction motif only plays a minor role in regulating the stability of Plk4 in these human cells.

The ubiquitination and degradation of Plk4<sup>AA</sup> (Fig. 2, D and F) suggested that phosphorylation of additional sites is required to promote Plk4's destruction. Therefore, mass spectrometry (MS) was used to map additional in vitro autophosphorylation sites on GST-Plk4<sup>WT</sup> (Fig. S3 A). A densely



**Figure 3. Plk4 autophosphorylates a 24-aa region to promote its own destruction.**

(A) Schematic showing the localization of the 24-aa region that is required for Plk4 to promote its own destruction. The alignment of this region, which is rich in potential phosphorylation sites (S/T residues), is shown. This putative  $\beta$ -TrCP-binding motif is contained within this region and marked by a line. (B) GST-Plk4 kinase assays were performed using His-Plk4<sup>KD</sup> (aa 1–416) as a substrate. GST-Plk4<sup>WT</sup> phosphorylates itself and His-Plk4<sup>KD</sup>, but note that phosphorylation of His-Plk4<sup>KD</sup> is reduced by the  $\Delta$ 24 mutation. Coomassie-stained gel shows the purified protein, and the autoradiogram shows the incorporation of  $\gamma$ [<sup>32</sup>P]ATP. Assays were performed for 60 min, and activity was measured by scintillation counting. (C) His-Plk4 (aa 1–416) kinase assay was performed using histone H1 as a substrate. Despite the fact that WT and  $\Delta$ 24 His-Plk4 have similar activity toward histone H1, His-Plk4 <sup>$\Delta$ 24</sup> displays reduced autophosphorylation. Coomassie-stained gel shows the purified protein, and autoradiogram shows the incorporation of  $\gamma$ [<sup>32</sup>P]ATP. Assays were performed for 60 min, and activity was measured by scintillation counting. (D) Immunoblot showing the relative expression levels of WT, AA,  $\Delta$ 24, and KD Plk4-EYFP. (E) Graph quantifying the proportion of cells with more than four centrioles 48 h after induction of Plk4-EYFP. (F) Graph quantifying the mean number of centrioles per cell in cells with more than four centrioles. Counting was performed 48 h after induction of Plk4-EYFP. (G) Immunofluorescence images acquired 48 h after Plk4-EYFP was induced. Insets depict an enlargement of centrioles. Red, SAS-6; green, Plk4-EYFP; blue, DNA. Bars, 10  $\mu$ m. C, Coomassie. Bars represent the mean of at least three independent experiments with >280 cells per condition. Error bars represent the SEM.



phosphorylated region containing 13 phosphorylatable aa within a 24-aa stretch (282–305) was identified (Fig. S3, B and C). This region contains the previously identified  $\beta$ -TrCP two-phosphosite phosphodegron (Cunha-Ferreira et al., 2009; Rogers et al., 2009) and is part of a putative PEST domain (aa 272–311) previously proposed to destabilize human Plk4 (Fig. 3 A; Yamashita et al., 2001). Nine peptides within the 282–305 region were identified with multiple (up to four) phosphorylations, albeit the exact positions of those sites could not be identified with certainty because of the close packing of phosphorylatable amino acids (Fig. S3, B and C). We next tested whether Plk4 could autophosphorylate this 24-aa domain in vitro. GST-Plk4<sup>WT</sup> readily phosphorylated His-Plk4<sup>KD</sup> (aa 1–416), but His-Plk4 <sup>$\Delta$ 24</sup> (lacking aa 282–305) accumulated 42% less phosphorylation (Fig. 3 B). Furthermore, although kinase-active His-Plk4<sup>WT</sup> and His-Plk4 <sup>$\Delta$ 24</sup> phosphorylated histone H1 with similar efficiency, autophosphorylation of

His-Plk4 <sup>$\Delta$ 24</sup> was reduced by about a third (36%) compared with that of His-Plk4<sup>WT</sup> (Fig. 3 C). Together, these data demonstrate that Plk4 multiply autophosphorylates a 24-aa region (aa 282–305) and that this region is not required for kinase activity in vitro.

We next tested whether aa 282–305 were involved in regulating Plk4 stability in cells. Importantly, deletion of aa 282–305 (Plk4 <sup>$\Delta$ 24</sup>) dramatically stabilized Plk4 (Fig. 3 D). Plk4 <sup>$\Delta$ 24</sup> induced centriole overduplication in ~75% of cells, and such cells contained a mean of ~17 centrioles per cell compared with about eight centrioles for cells expressing Plk4<sup>WT</sup> (Fig. 3, E–G). This suggests that Plk4 multiply autophosphorylates a 24-aa phosphodegron (282–305) that is required to destabilize kinase-active Plk4.

To determine how phosphorylation contributes to the instability of kinase-active Plk4, we created several Plk4 mutants that were defective in phosphorylation at specific sites within aa 282–305 (Fig. 4 A): Plk4<sup>AA</sup> contains two mutations in the

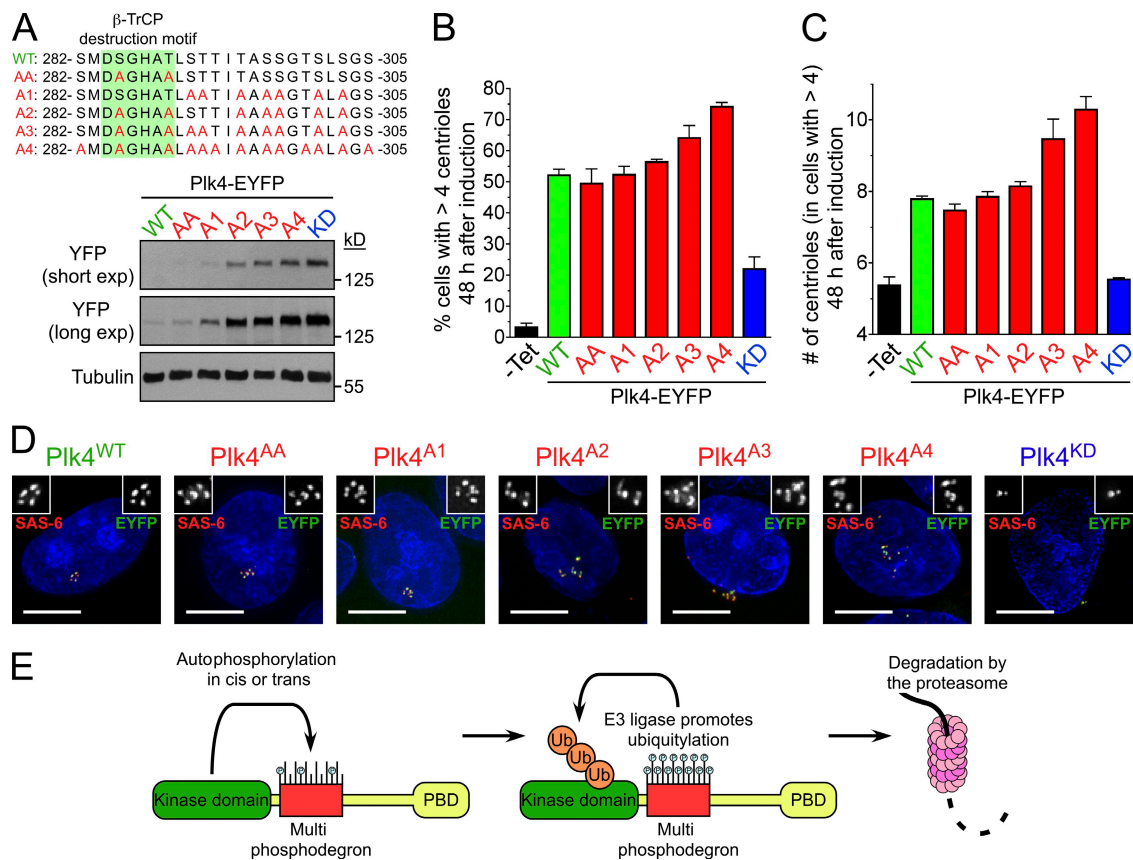


**Figure 4. Phosphorylation of multiple sites is required for optimal Plk4 destruction.** (A) Alignment showing the positions of the different phosphorylation mutations in Plk4. Immunoblot showing the relative expression levels of WT, AA, A1, A2, A3, A4, and KD Plk4-EYFP. (B) Graph quantifying the proportion of cells with more than four centrioles 48 h after induction of Plk4-EYFP. Uninduced samples (–Tet) are shown for comparison. (C) Graph quantifying the mean number of centrioles per cell in cells with more than four centrioles. Counting was performed 48 h after induction of Plk4-EYFP. Uninduced samples are shown for comparison. (D) Immunofluorescence images acquired 48 h after Plk4-EYFP was induced. Insets depict an enlargement of centrioles. Red, SAS-6; green, Plk4-EYFP; blue, DNA. Bars, 10  $\mu$ m. (E) A model for the autoregulation of Plk4 stability. Bars represent the mean of at least three independent experiments with >300 cells per condition. Error bars represent the SEM.

$\beta$ -TrCP phosphodegron, Plk4<sup>A1</sup> possesses mutations in the seven most-conserved phosphorylation sites downstream of the  $\beta$ -TrCP phosphodegron, Plk4<sup>A2</sup> contains mutations in the  $\beta$ -TrCP phosphodegron and five downstream phosphorylation sites, Plk4<sup>A3</sup> has nine phosphorylation sites mutated, and Plk4<sup>A4</sup> has all 13 phosphorylation sites abolished. Expression of these mutants in cells revealed that Plk4 became progressively stabilized as more phosphorylation sites were abolished (Fig. 4 A). The stability of the various Plk4 phosphorylation mutants closely mirrored their capacity to drive centriole overduplication in cells, with both the proportion of cells with supernumerary centrioles and the numbers of centrioles per cell increasing as more phosphorylation sites were mutated (Fig. 4, B–D). These data imply that autophosphorylation within aa 282–305 has an additive effect on promoting Plk4's destruction and acts to self-limit Plk4 activity and centriole duplication in cells.

Together, our results show that Plk4's kinase activity autoregulates Plk4 protein stability. Our data do not exclude the possibility that Plk4 activity regulates stability through additional proteins; for example, Plk4-induced activation of an unknown kinase may regulate Plk4 stability. However, we demonstrate that Plk4 is capable of autophosphorylating a region crucial for the kinase activity-dependent degradation of Plk4. Therefore,

we favor the interpretation that Plk4 directly promotes its own destruction through autophosphorylation of a 13-site multiphosphodegron (Fig. 4 E). The multiphosphodegron possesses a conserved  $\beta$ -TrCP-binding site previously implicated in regulating the stability of *Drosophila* Plk4 (Cunha-Ferreira et al., 2009; Rogers et al., 2009). A mutant of mouse Plk4 unable to be phosphorylated in the  $\beta$ -TrCP-binding site (Plk4<sup>AA</sup>) exhibited dramatically reduced  $\beta$ -TrCP binding; however, Plk4<sup>AA</sup> was ubiquitinated and only modestly stabilized in cells. In contrast, deletion of the entire 24-aa multiphosphodegron or mutation of all 13 phosphorylation sites in this region dramatically stabilized Plk4, suggesting that autophosphorylated Plk4 interacts with additional SCF F box proteins or alternative E3 ubiquitin ligases that are required for degradation. Surprisingly, we found that repression of  $\beta$ -TrCP stabilized Plk4<sup>AA</sup>, indicating that SCF <sup>$\beta$ -TrCP</sup> still contributes to the destruction of this mutant (Fig. S3 D). Although we suspect that this arises from an indirect effect of  $\beta$ -TrCP depletion, it is possible that the small amounts of  $\beta$ -TrCP associated with Plk4<sup>AA</sup> still play a role in targeting the protein for destruction.

Because Plk4 phosphorylation occurs in dynamic equilibrium with counteracting phosphatases, we speculate that a requirement for multisite phosphorylation to prime degradation is

likely to provide a temporal delay to allow Plk4 to phosphorylate critical substrates required for centriole duplication before its protein level is down-regulated. This could create a sensitive biological switch in which Plk4 can be rapidly destabilized once its activity reaches a certain threshold level. This autoregulatory feedback loop places Plk4 stability under direct control of its own activity and may form an important mechanism to limit normal centriole duplication to once per cell cycle.

## Materials and methods

### Constructs

The full-length mouse Plk4 open reading frame was cloned into a pcDNA5/FRT/TO-based vector (Invitrogen) modified to contain a C terminus EYFP or Myc epitope tag. To create Plk4<sup>A1</sup> and Plk4<sup>A4</sup>, two silent point mutations were introduced to create an NheI site at aa 225–226. A fragment of mouse Plk4 (aa 223–387) encoding the appropriate mutations was synthesized (Genscript) and used to replace a corresponding NheI–XhoI fragment in mouse Plk4. All other Plk4 mutants were generated by site-directed mutagenesis (QuickChange; Agilent Technologies). To create His-Plk4 (aa 1–416), the first 416 aa of mouse Plk4 were amplified by PCR and cloned into a pET30 bacterial expression vector (EMD), which contains an N-terminal 6His tag. To create GST-Plk4, the mouse Plk4 open reading frame was cloned into a pFastBac1 (Invitrogen)-based vector modified to contain an N terminus GST tag. pcDNA3 Myc-β-TrCP and pcDNA3 HA-ubiquitin plasmids were obtained from Addgene.

### Cell culture

Cells were maintained at 37°C in a 5% CO<sub>2</sub> atmosphere in DME containing 10% tetracycline-free FBS (Takara Bio Inc.), 100 U/ml penicillin, 100 U/ml streptomycin, and 2 mM L-glutamine. DLD-1 cells were used in all experiments except in Fig. 2 (E and F), which used HEK 293 cells.

### Generation of stable cell lines and siRNA treatment

RFP-tagged histone H2B (H2B-RFP) was introduced into Flp-In TRex-DLD-1 parental cells (provided by S. Taylor, The University of Manchester, Manchester, England, UK) using retroviral delivery as described previously (Shah et al., 2004). Stable integrates were selected in 2 μg/ml puromycin, and single clones were isolated using FACS (FACS Advantage; BD). Stable, isogenic cell lines expressing Plk4-EYFP were generated using the FRT/Flp-mediated recombination as described previously (Tighe et al., 2004). Expression of Plk4-EYFP was induced with 1 μg/ml tetracycline (Sigma-Aldrich). Flp-In TRex-DLD-1 H2B-RFP cells were used for all the experiments except in Fig. 2 (E and F). Small molecules were used at the following final concentrations: nocodazole MG132 (EMD), 20 μM; 1NM-PP1 (EMD), 10 μM. For siRNA treatment, 1.5 × 10<sup>5</sup> cells were plated in a 6-well plate, and duplexed siRNAs were introduced using Oligofectamine (Invitrogen). siRNAs directed against β-TrCP (5'-GUGGAUUUGUGGAACAUC-3') and GAPDH (5'-UGGUUUACAUGAUCCAAUA-3') were purchased from Thermo Fisher Scientific. 24 h after transfection, tetracycline was added to induce expression of Plk4-EYFP and cells harvested and processed for immunoblotting 24 h later.

### Immunoblotting and immunofluorescence

To purify Plk4-YFP, cells were lysed in lysis buffer (10 mM Tris, pH 7.5, 0.1% Triton X-100, 100 mM NaCl, 1 mM EDTA, 1 mM EGTA, 50 mM NaF, 20 mM β-glycerophosphate, 0.1 mM DTT, 200 nM microcystin, 1 mM PMSF, and 1 μM leupeptin, pepstatin, and chymostatin [LPC]), sonicated, and soluble extracts were prepared. The supernatant was incubated with beads alone or beads coupled to GFP-binding protein (GBP; Rothbauer et al., 2008). Beads were washed five times in lysis buffer, and protein complexes were analyzed by immunoblotting. For immunoblot analysis, protein samples were separated by SDS-PAGE, transferred onto nitrocellulose membranes (Bio-Rad Laboratories), and probed with antibodies 4A6 (mouse anti-Myc; 1:1,000; Millipore), DM1A (mouse anti-α-tubulin; 1:1,000), and YFP (mouse anti-GFP; 1:500; Roche). For immunofluorescence, cells were grown on hydrochloric acid-washed, poly-L-lysine (Sigma-Aldrich)-coated 18-mm glass coverslips and fixed in 100% ice-cold methanol for 10 min. Cells were blocked in 2.5% FBS, 200 mM glycine, and 0.1% Triton X-100 in PBS for 1 h. Antibody incubations were conducted in the blocking solution for 1 h. DNA was detected using DAPI, and cells were mounted in Prolong Antifade (Invitrogen).

Staining was performed with antibodies SAS-6 (human anti-SAS-6; provided by A. Dammermann, Ludwig Institute for Cancer Research, San Diego, CA) and GTU-88 (mouse anti-γ-tubulin; 1:250; Abcam). YFP was visualized directly using a GFP filter set, the human SAS6 antibody was directly conjugated to Cy5 (Jackson ImmunoResearch Laboratories, Inc.), and GTU88 was stained with a secondary goat anti-mouse antibody conjugated to AMCA.

Immunofluorescence images were collected using an inverted microscope (IX-70; Olympus) with a Deltavision Core system (Applied Precision) controlling an interline charge-coupled device camera (CoolSNAP; Roper Industries) driven by softWoRx software (Applied Precision). Images were collected using a 100× or 60× 1.4 NA oil objective (Olympus) at 0.2-μm z sections and subsequently deconvolved. Imaging was performed at room temperature, and maximum intensity 2D projections were assembled for each image using softWoRx. With the exception of the images in Fig. S1 E, EYFP exposure times were adjusted for each Plk4-EYFP mutant. Centriole numbers were determined by counting the number of structures that stained positive for both Plk4-EYFP and SAS-6. For quantitation of EYFP, signal intensity at the centriole unconvolved 2D maximum-intensity projections was saved as unscaled 16-bit TIFF images. Signal intensity was determined using MetaMorph (MDS Analytical Technologies) by drawing a 20 × 20-pixel box and a larger 25 × 25-pixel box around the centrosome. The integrated EYFP intensity in the smaller box was calculated by subtracting the mean fluorescence intensity in the area between the two boxes (mean background) from the mean GFP intensity in the smaller box and multiplying by the area of the smaller box.

### Protein purification

GBP was purified from *Escherichia coli* (strain Rosetta [DE3]) and covalently coupled to NHS-activated Sepharose 4 Fast Flow beads (GE Healthcare) at 1 mg/ml as described previously (Rothbauer et al., 2008). Recombinant His-Plk4 (aa 1–416) was transformed in *E. coli* (strain Rosetta [DE3]), and protein expression was induced at 16°C for 18 h with 200 nM IPTG. Bacterial pellets were suspended in lysis buffer (50 mM Tris-HCl, pH 8.0, 100 mM NaCl, 20 mM imidazole, 0.1% β-mercaptoethanol, 0.1% NP-40, 1 mM PMSF, and 1 μM LPC) and lysed by sonication after 1 mg/ml lysozyme treatment on ice for 30 min. After centrifugation at 15,000 rpm (SA-600; Sorvall) for 30 min, the supernatant was incubated with pre-washed nickel nitrilotriacetic acid beads (QIAGEN) for 1 h at 4°C. Beads were washed extensively in wash buffer (50 mM Tris-HCl, pH 8.0, 500 mM NaCl, 20 mM imidazole, 0.1% β-mercaptoethanol, 0.1% NP-40, 1 mM PMSF, and 1 μM LPC), and protein was eluted in elution buffer (50 mM Tris-HCl, pH 8.0, 100 mM NaCl, 300 mM imidazole, 0.1% β-mercaptoethanol, and 0.1% NP-40). Proteins were dialyzed into a final buffer containing 50 mM Tris-HCl, pH 8.0, 100 mM NaCl, 20 mM imidazole, and 0.1% β-mercaptoethanol. Recombinant GST-Plk4 was expressed and purified from insect cells (High Five; Invitrogen) using the Bac-to-Bac expression system (Invitrogen). Infected cell pellets were suspended in lysis buffer (PBS supplemented with 2 mM MgCl<sub>2</sub>, 5 mM DTT, 10 nM microcystin, 1 mM Na<sub>3</sub>VO<sub>4</sub>, 250 U benzamide nuclease [Sigma-Aldrich], 1 mM PMSF, and 1 mM LPC) and lysed by sonication. After centrifugation at 15,000 rpm (SA-600; Sorvall) for 30 min, the supernatant was supplemented with 110 mM KCl and 0.1% Triton X-100 and incubated with glutathione Sepharose (GE Healthcare) for 1 h at 4°C. Beads were washed extensively in wash buffer (PBS supplemented with 1 mM DTT, 0.1% Triton X-100, 100 mM KCl, 1 mM PMSF, and 1 μM LPC), and protein was eluted in elution buffer (1× PBS supplemented with 40 mM reduced glutathione, 50 mM Tris, pH 8.0, and 5 mM DTT).

### In vitro kinase assays

In vitro kinase assays were performed at room temperature in 20 mM Tris, pH 7.5, 25 mM KCl, 10 mM MgCl<sub>2</sub>, 1 mM DTT, 5 μM Na<sub>3</sub>VO<sub>4</sub> in the presence of 50 μM ATP, and 100 μCi/ml [γ-<sup>32</sup>P]ATP. 2 μg of substrate was incubated with 1 μg purified GST-Plk4 or 2 μg His-Plk4 (aa 1–416). Kinase reactions were stopped with sample buffer and analyzed by SDS-PAGE. For quantification, individual bands were excised, and the incorporation of <sup>32</sup>P was quantified using a scintillation counter (Beckman Coulter). For λ phosphatase treatment, GST-Plk4 was incubated with λ phosphatase (New England Biolabs, Inc.) at 30°C for 30 min.

### MS sample preparation

20 μg trichloroacetic acid-precipitated GST-Plk4<sup>WT</sup> was dissolved in 8 M urea and 100 mM Tris, pH 8.0, with a final volume of 25 μl. The protein was reduced in 5 mM TCEP (Fluka) for 20 min at room temperature and alkylated in 10 mM iodoacetamide (Sigma-Aldrich) for 15 min in the dark. Each sample was diluted fourfold with 100 mM Tris, pH 8.0, and CaCl<sub>2</sub>.



was added to a final concentration of 1 mM. 0.8  $\mu$ l trypsin (0.5  $\mu$ g/ $\mu$ l; Promega) was added for an overnight digestion at 37°C. Samples were acidified with formic acid to a final concentration of 5% for MS analysis.

## MS analysis

The tryptic digest was pressure loaded onto an equilibrated fused silica capillary column containing 3 cm Aqua 5u C18 (Phenomenex) packed into a 250- $\mu$ m-i.d. capillary with a filtered union (Upchurch Scientific). Next, an equilibrated 100- $\mu$ m-i.d capillary with a 5- $\mu$ m pulled tip containing 10 cm of C18 material was attached to the filter union and placed in line with a quaternary HPLC (1200; Agilent Technologies). Peptides were separated with a 2-h organic gradient (Dix et al., 2008) and analyzed on an LTQ-Orbitrap as previously described (Lu et al., 2008), except one full Fourier transform scan mass spectrum (400–1,800 m/z; resolution of 60,000) was followed by nine data-dependent MS/MS acquired in the linear ion trap.

## Analysis of MS data

The ms<sup>2</sup> spectra data were extracted from the raw files using the publicly available RAW Xtractor (version 1.9.1). Ms<sup>2</sup> spectra data were searched using the ProLuCID search algorithm (Xu, T., J.D. Venable, S. Kyu Park, D. Cociorva, B. Lu, L. Liao, J. Wohlschlegel, J. Hewel, and J.R. Yates III. 2006. Human Proteome Organisation Fifth Annual World Congress. Abstr. S271) against a custom-made database containing the longest entry form of the mouse International Protein Index database (version 3.26) associated with each Ensembl gene identifier, resulting in a total of 22,833 unique entries. Additionally, each of these entries was reversed and appended to the database for assessment of false-positive rates. In total, the search database contained 45,666 protein sequence entries (22,833 real sequences and 22,833 decoy sequences). Searches allowed for the static modification of cysteine residues (57.02146 D; because of alkylation) and differential modification (79.9663 D; phosphorylation) on serine and threonine residues up to a maximum of four residues per peptide. In addition, full tryptic enzyme specificity was defined for searches with a mass tolerance set to 100 ppm for precursor mass and 600 ppm for product ion masses. The resulting ms<sup>2</sup> spectra matches were assembled and filtered using DTASelect2 (version 2.0.27). For this analysis, modified and unmodified peptides were each individually evaluated using the DTASelect2 software. In each of these subgroups, the distribution of Xcorr and DeltaCN values for a direct (to the direct database) and decoy (reversed database) were separated by quadratic discriminant analysis. Spectral matches were retained with Xcorr and deltaCN values that produced a maximum peptide false-positive rate of 1% that was derived from the frequency of matches to the decoy reverse database (number of decoy database hits/number of filtered peptides identified  $\times$  100). This value is calculated by the DTASelect2 software. In addition, a minimum peptide length of 6-aa residues was imposed. Such criteria resulted in the elimination of most decoy database hits. Modified peptides were further validated using Debunker (Lu et al., 2007).

## Online supplemental material

Fig. S1 shows that kinase activity destabilizes centriole-localized Plk4. Fig. S2 shows that an AS mutant of recombinant Plk4 can be inhibited with the ATP analogue 1NM-PP1. Fig. S3 shows in vitro phosphorylation analysis of recombinant GST-Plk4. Online supplemental material is available at <http://www.jcb.org/cgi/content/full/jcb.200911102/DC1>.

We thank Edward Yeh for depositing pcDNA3 HA-ubiquitin and Yue Xiong for depositing pcDNA3 Myc- $\beta$ -TrCP in the Addgene plasmid repository. We also thank Stephen Taylor and Alexander Dammermann for providing reagents for this study.

This work was supported by a grant (GM29513) from the National Institutes of Health to D.W. Cleveland, who receives salary support from the Ludwig Institute for Cancer Research. A.J. Holland was supported by a European Molecular Biology Organization Long-Term Fellowship.

Submitted: 19 November 2009

Accepted: 23 December 2009

## References

Basto, R., K. Brunk, T. Vinadogrova, N. Peel, A. Franz, A. Khodjakov, and J.W. Raff. 2008. Centrosome amplification can initiate tumorigenesis in flies. *Cell*. 133:1032–1042. doi:10.1016/j.cell.2008.05.039

Bettencourt-Dias, M., A. Rodrigues-Martins, L. Carpenter, M. Riparbelli, L. Lehmann, M.K. Gatt, N. Carmo, F. Balloux, G. Callaini, and D.M. Glover.

2005. SAK/PLK4 is required for centriole duplication and flagella development. *Curr. Biol.* 15:2199–2207. doi:10.1016/j.cub.2005.11.042

Bishop, A.C., J.A. Ubersax, D.T. Petsch, D.P. Matheos, N.S. Gray, J. Blethrow, E. Shimizu, J.Z. Tsien, P.G. Schultz, M.D. Rose, et al. 2000. A chemical switch for inhibitor-sensitive alleles of any protein kinase. *Nature*. 407:395–401. doi:10.1038/35030148

Burkard, M.E., C.L. Randall, S. Laroche, C. Zhang, K.M. Shokat, R.P. Fisher, and P.V. Jallepalli. 2007. Chemical genetics reveals the requirement for Polo-like kinase 1 activity in positioning RhoA and triggering cytokinesis in human cells. *Proc. Natl. Acad. Sci. USA*. 104:4383–4388. doi:10.1073/pnas.0701140104

Castellanos, E., P. Dominguez, and C. Gonzalez. 2008. Centrosome dysfunction in *Drosophila* neural stem cells causes tumors that are not due to genome instability. *Curr. Biol.* 18:1209–1214. doi:10.1016/j.cub.2008.07.029

Cunha-Ferreira, I., A. Rodrigues-Martins, I. Bento, M. Riparbelli, W. Zhang, E. Laue, G. Callaini, D.M. Glover, and M. Bettencourt-Dias. 2009. The SCF/Slimb ubiquitin ligase limits centrosome amplification through degradation of SAK/PLK4. *Curr. Biol.* 19:43–49. doi:10.1016/j.cub.2008.11.037

Dix, M.M., G.M. Simon, and B.F. Cravatt. 2008. Global mapping of the topography and magnitude of proteolytic events in apoptosis. *Cell*. 134:679–691. doi:10.1016/j.cell.2008.06.038

Duensing, A., Y. Liu, S.A. Perdreau, J. Kleylein-Sohn, E.A. Nigg, and S. Duensing. 2007. Centriole overduplication through the concurrent formation of multiple daughter centrioles at single maternal templates. *Oncogene*. 26:6280–6288. doi:10.1038/sj.onc.1210456

Fode, C., C. Binkert, and J.W. Dennis. 1996. Constitutive expression of murine Sak-a suppresses cell growth and induces multinucleation. *Mol. Cell Biol.* 16:4665–4672.

Frescas, D., and M. Pagano. 2008. Deregulated proteolysis by the F-box proteins SKP2 and beta-TrCP: tipping the scales of cancer. *Nat. Rev. Cancer*. 8:438–449. doi:10.1038/nrc2396

Ganem, N.J., S.A. Godinho, and D. Pellman. 2009. A mechanism linking extra centrosomes to chromosomal instability. *Nature*. 460:278–282. doi:10.1038/nature08136

Guardavaccaro, D., Y. Kudo, J. Boulaire, M. Barchi, L. Busino, M. Donzelli, F. Margottin-Goguet, P.K. Jackson, L. Yamasaki, and M. Pagano. 2003. Control of meiotic and mitotic progression by the F box protein beta-Trcp1 in vivo. *Dev. Cell*. 4:799–812. doi:10.1016/S1534-5807(03)00154-0

Habedanck, R., Y.D. Stierhof, C.J. Wilkinson, and E.A. Nigg. 2005. The Polo kinase Plk4 functions in centriole duplication. *Nat. Cell Biol.* 7:1140–1146. doi:10.1038/ncb1320

Holland, A.J., and D.W. Cleveland. 2009. Boveri revisited: chromosomal instability, aneuploidy and tumorigenesis. *Nat. Rev. Mol. Cell Biol.* 10:478–487. doi:10.1038/nrm2718

Ko, M.A., C.O. Rosario, J.W. Hudson, S. Kulkarni, A. Pollett, J.W. Dennis, and C.J. Swallow. 2005. Plk4 haploinsufficiency causes mitotic infidelity and carcinogenesis. *Nat. Genet.* 37:883–888. doi:10.1038/ng1605

Korzeniewski, N., L. Zheng, R. Cuevas, J. Parry, P. Chatterjee, B. Anderton, A. Duensing, K. Munger, and S. Duensing. 2009. Cullin 1 functions as a centrosomal suppressor of centriole multiplication by regulating polo-like kinase 4 protein levels. *Cancer Res.* 69:6668–6675. doi:10.1158/0008-5472.CAN-09-1284

Lengauer, C., K.W. Kinzler, and B. Vogelstein. 1997. Genetic instability in colorectal cancers. *Nature*. 386:623–627. doi:10.1038/386623a0

Loncerek, J., and A. Khodjakov. 2009. Ab ovo or de novo? Mechanisms of centriole duplication. *Mol. Cells*. 27:135–142. doi:10.1007/s10059-009-0017-z

Lu, B., C. Ruse, T. Xu, S.K. Park, and J. Yates III. 2007. Automatic validation of phosphopeptide identifications from tandem mass spectra. *Anal. Chem.* 79:1301–1310. doi:10.1021/ac061334v

Lu, B., A. Motoyama, C. Ruse, J. Venable, and J.R. Yates III. 2008. Improving protein identification sensitivity by combining MS and MS/MS information for shotgun proteomics using LTQ-Orbitrap high mass accuracy data. *Anal. Chem.* 80:2018–2025. doi:10.1021/ac701697w

Macmillan, J.C., J.W. Hudson, S. Bull, J.W. Dennis, and C.J. Swallow. 2001. Comparative expression of the mitotic regulators SAK and PLK in colorectal cancer. *Ann. Surg. Oncol.* 8:729–740. doi:10.1007/s10434-001-0729-6

Nigg, E.A. 2002. Centrosome aberrations: cause or consequence of cancer progression? *Nat. Rev. Cancer*. 2:815–825. doi:10.1038/nrc924

Nigg, E.A. 2006. Origins and consequences of centrosome aberrations in human cancers. *Int. J. Cancer*. 119:2717–2723. doi:10.1002/ijc.22245

Peel, N., N.R. Stevens, R. Basto, and J.W. Raff. 2007. Overexpressing centriole-replication proteins in vivo induces centriole overduplication and de novo formation. *Curr. Biol.* 17:834–843. doi:10.1016/j.cub.2007.04.036

Rogers, G.C., N.M. Rusan, D.M. Roberts, M. Peifer, and S.L. Rogers. 2009. The SCF<sup>Slimb</sup> ubiquitin ligase regulates Plk4/Sak levels to block centriole reduplication. *J. Cell Biol.* 184:225–239. doi:10.1083/jcb.200808049

- Rothbauer, U., K. Zolghadr, S. Muyldermans, A. Schepers, M.C. Cardoso, and H. Leonhardt. 2008. A versatile nanotrap for biochemical and functional studies with fluorescent fusion proteins. *Mol. Cell. Proteomics*. 7:282–289.
- Shah, J.V., E. Botvinick, Z. Bonday, F. Furnari, M. Berns, and D.W. Cleveland. 2004. Dynamics of centromere and kinetochore proteins; implications for checkpoint signaling and silencing. *Curr. Biol.* 14:942–952.
- Silkworth, W.T., I.K. Nardi, L.M. Scholl, and D. Cimini. 2009. Multipolar spindle pole coalescence is a major source of kinetochore mis-attachment and chromosome mis-segregation in cancer cells. *PLoS One*. 4:e6564. doi:10.1371/journal.pone.0006564
- Swallow, C.J., M.A. Ko, N.U. Siddiqui, J.W. Hudson, and J.W. Dennis. 2005. Sak/Plk4 and mitotic fidelity. *Oncogene*. 24:306–312. doi:10.1038/sj.onc.1208275
- Tighe, A., V.L. Johnson, and S.S. Taylor. 2004. Truncating APC mutations have dominant effects on proliferation, spindle checkpoint control, survival and chromosome stability. *J. Cell Sci.* 117:6339–6353. doi:10.1242/jcs.01556
- Yamashita, Y., S. Kajigaya, K. Yoshida, S. Ueno, J. Ota, K. Ohmine, M. Ueda, A. Miyazato, K. Ohya, T. Kitamura, et al. 2001. Sak serine-threonine kinase acts as an effector of Tec tyrosine kinase. *J. Biol. Chem.* 276:39012–39020. doi:10.1074/jbc.M106249200